Preliminary results from the second flight of CREAM

P.S. Marrocchesi [d,*], H.S. Ahn [a], P. Allison [c], M.G. Bagliesi [d], L. Barbier [j], J.J. Beatty [c], G. Bigongiari [d], T.J. Brandt [c], J.T. Childers [e], N.B. Conklin [f], S. Coutu [f], M.A. DuVernois [e], O. Ganel [a], J.H. Han [a], J.A. Jeon [g], K.C. Kim [a], M.H. Lee [a], L. Lutz [a], P. Maestro [d], A. Malinine [a], S. Minnick [h], S.I. Mognet [f], S.W. Nam [g], S. Nutter [i], I.H. Park [g], N.H. Park [g], E.S. Seo [a,b], R. Sina [a], P. Walpole [a], J. Wu [a], J. Yang [g], Y.S. Yoon [b], R. Zei [d], S.Y. Zinn [a]

[a] Institute for Physical Science and Technology, University of Maryland, College Park, MD 20742, USA
[b] Department of Physics, University of Maryland, College Park, MD 20742, USA
[c] Department of Physics, Ohio State University, Columbus, OH 43210, USA
[d] Department of Physics, University of Siena and INFN, Via Roma 56, 53100 Siena, Italy
[e] School of Physics and Astronomy, University of Minnesota, Minneapolis, MN 55455, USA
[f] Department of Physics, Penn State University, University Park, PA 16802, USA
[g] Department of Physics, Ewha Womans University, Seoul 120-750, Republic of Korea
[h] Department of Physics, Kent State University Tuscarawas, New Philadelphia, OH 44663, USA
[i] Department of Physics and Geology, Northern Kentucky University, Highland Heights, KY 41099, USA
[j] Goddard Space Flight Center, 8800 Greenbelt Road, Greenbelt, MD 20771, USA

Abstract

Launched from McMurdo (Antarctica) in December 2005, the balloon experiment CREAM (cosmic ray energetics and mass) collected about 15 million triggers during its second flight of 28 days. Redundant charge identification, by two pixelated silicon arrays and a time resolved pulse shaping technique from a scintillator system, allowed a clear signature of the primary nuclei. The energy was measured with a tungsten/SciFi calorimeter preceded by a graphite target. Preliminary results from the analysis of the data of the second flight are presented.
© 2008 Published by Elsevier Ltd on behalf of COSPAR.

Keywords: Cosmic ray; Balloon measurements

1. Introduction

CREAM (cosmic ray energetics and mass) is a balloon experiment designed to perform direct measurements of cosmic ray composition and energy spectra above the atmosphere. The goal of this multi-mission experiment is to collect, in a series of flights, sufficient statistics to explore the region of energies up to 10^{15} eV and test the current models of cosmic ray acceleration and propagation in the Galaxy. Two instrument suites were built to be flown from Antarctica on alternate years. In this way, the refurbishment operations that follow the recovery of one payload could take place almost simultaneously with the flight preparation of the second payload. The CREAM-1 instrument, flown for the first time in December 2004 with a conventional zero-pressure balloon, achieved a record-breaking flight duration of 42 days (Seo, 2005). The second CREAM payload was launched from McMurdo in December 2005 and its flight lasted 28 days (Seo et al., 2006). The balloon circumnavigated the Antarctic continent twice and floated at an altitude between 35 and 40 km with an atmospheric overburden of 3–4 g/cm^2. The CREAM-1

---

instrument (Seo et al., 2004) included a sampling tungsten/scintillating fiber calorimeter preceded by a graphite target with scintillating fiber hodoscopes, a pixelated silicon charge detector (SCD), a transition radiation detector (TRD) and a segmented timing-based particle-charge detector (TCD). The CREAM-2 instrument configuration did not include the TRD and scintillating fiber hodoscopes as in the first flight, while the charge identification performances of SCD were enhanced by the addition of a second layer of pixelated silicon sensors. In this paper, preliminary results of the analysis of the data from the second flight are reported.

2. Science perspectives with CREAM

One of the main physics goals driving the CREAM investigation (Seo et al., 2004) is the experimental test of the validity of models based on cosmic ray (CR) acceleration by supernova shock waves. In a class of such models, a rigidity dependent critical energy is derived, which marks the limit where diffusive shock acceleration becomes inefficient. In this scenario, the spectral break ("knee"), observed in the all-particle spectrum, would be the combined result of a Z-dependent cut-off in the spectrum of each element present in the cosmic ray flux. As a consequence, the CR elemental composition is predicted to change with energy with a depletion of low-Z nuclei at higher energy.

While early models (Lagage and Cesarsky, 1983) favoured a maximum energy for supernova acceleration at a scale of order $Z \times 10^{14}$ eV for a nucleus of atomic number Z, a variety of more recent theoretical approaches to the problem of cosmic ray acceleration (for a recent review see, for instance, Hillas (2005)) broadens the spectrum of theoretical predictions. For protons, for instance, a possible spectral break might be located at energies ranging from 100 TeV to a few PeV.

A common feature of all models is their capability to predict the detailed shape of the energy spectrum of each element (Biermann, 1993). Therefore, experiments designed to discriminate among different models, have to provide an unambiguous identification of the incoming particle (via a precise measurement of its charge) and a sufficiently accurate determination of its energy. The search for a possible cutoff in the spectra of light nuclei and the consequent change in the elemental composition of cosmic rays, as a function of energy, is one of the main science goals of CREAM. Furthermore, the instrument can be used to assess possible differences in the spectral slopes of heavier nuclei with respect to helium and to protons. Recent high energy data from the ATIC balloon experiment on proton and He spectra (Wefel et al., 2005) clearly indicate the interest to investigate in more detail the difference in the energy dependence of the spectra of the two lightest nuclei. Another broad science objective, addressed by CREAM, is the measurement of the spectra of secondary elements up to the highest possible energies allowed by the irreducible background, generated by the residual atmospheric over-

burden at balloon altitudes. The aim is to get a consistent picture of the propagation of cosmic rays through the Galaxy and of their interactions with the interstellar medium. Measurements of secondary-to-primary ratios (Swordy, 2001) would allow the determination of the parameter δ whose value is critical to discriminate among different models (Ptuskin, 1996; Berezhko et al., 2003) predicting a possible $E^{-\delta}$ energy dependence for the propagation path-length. Once the value of this parameter is known with sufficient accuracy, it will be possible to infer the shape of the acceleration spectra of individual elements at the source.

The CREAM instrument was designed to provide a redundant charge identification by means of dedicated detectors using different techniques (Cherenkov light, specific ionization in scintillators, silicon sensors or gas proportional tubes). A redundant energy measurement was provided by means of two different subdetectors: a calorimeter with an energy threshold below 1 TeV and an almost energy independent resolution up to about 1 PeV, and a transition radiation energy meter for $Z > 3$ nuclei, with a threshold close to 500 GeV/n and saturation around 20 TeV/n.

During the first flight, due to the large geometric factor of the TRD (with a trigger aperture close to 2.2 m^2 sr), the CREAM instrument configuration allowed to collect a large sample of high-Z nuclei, for the study of the spectra of secondary nuclei and to measure the energy dependence of secondary-to-primary ratios (most notably boron to carbon). For heavy nuclei studies, the geometry factor of the CREAM-2 flight configuration is smaller, being limited by the acceptance of the calorimeter module. On the other hand, the instrument features an enhanced charge discrimination (with one additional SCD layer) and it is therefore more suited for studies of the spectral features of light nuclei.

3. Instrument performance during the second flight

The main detector subsystems, from bottom to top of the instrument, are briefly described in the following, together with a summary of their flight performance.

3.1. The imaging calorimeter

The calorimeter is preceded by a $\sim$0.5 λ_{int} thick graphite target to induce inelastic interactions of the incident nucleus. The narrow electromagnetic core of the hadronic shower is 3D-imaged by a finely segmented sampling calorimeter (Marrocchesi et al., 2004), built as a stack of 20 tungsten plates, interleaved with active planes of 1 cm wide, 50 cm long, scintillating fibers ribbons. The active area of the detector is 50×50 cm^2, with lateral segmentation corresponding to about 1 Moliere radius. The layers of scintillating fiber ribbons are alternatively oriented along the X and Y directions to image the longitudinal and lateral shower development and to provide the direction of the incident particle, via the reconstruction of the shower axis (Fig. 1).
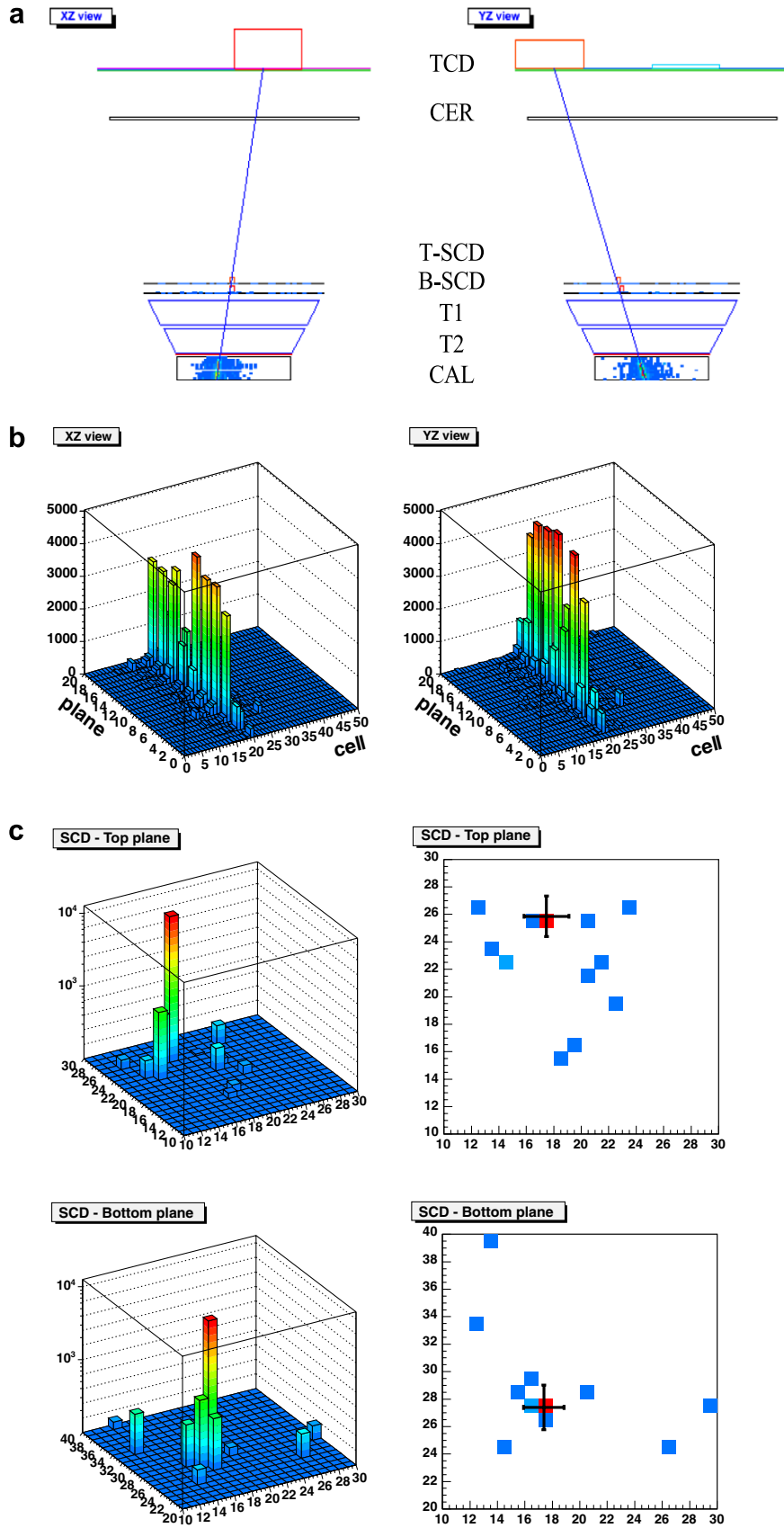
Fig. 1. (a) Event display of a candidate Fe nucleus detected by the CREAM-2 instrument; (b) two orthogonal views of the shower image in the calorimeter (the vertical axis is in MeV); (c) left: signals from individual pixels in the lower and upper SCD layers (the vertical scale in the lego plot is in ADC counts, where one MIP corresponds to about 35 counts); right: zoomed view around the selected pixel with the impact point of the track extrapolation drawn with its error. The x and y axis coordinates identify the pixel position.

The light signal from each ribbon is collected by means of an acrylic light-mixer coupled to a bundle of clear fibers. This is split into 3 sub-bundles, each feeding a pixel of a hybrid photo diode (HPD). In this way the wide dynamic range of the calorimeter is divided into 3 sub-ranges (LOW, MID, HI) with different gain, chosen to match the dynamic range of the front-end electronics. A total of 2560 channels are readout from 40 photodetectors arranged in 4 crates and powered in groups of 5 units.

3.1.1. High voltage and thermal behaviour

The hybrid photodetectors of the calorimeter require an operational voltage of several kV. The system has to operate at low atmospheric pressure (a few mbar) as the payload is not pressurized (Ganel et al., 2001). During the flight, the calorimeter high voltage system performed successfully with an average voltage setting at 7 kV. An exception was the HV trip of one module on December 23rd. The high voltage was promptly restored at a lower voltage of 6 kV and finally set to the original value. Temperature sensors monitored the calorimeter's thermal behaviour, that was found in good agreement with the expectations of the flight thermal model, with an operative temperature range between 20 and 35 °C, for the electronics crates located on the sun-side, and 15–30 °C for those on the anti-sun side. A daily temperature fluctuation of about 10 °C was observed, depending on the inclination of the sun light during each 24-h cycle.

3.1.2. Front-end electronics behaviour

The behaviour of the photodetectors and front-end electronics of the calorimeter was monitored during the whole flight, by means of special calibration runs repeated every 2 h: the HPD response stability was checked by illuminating a few pixels with LED light, while the electronics channels variations were monitored by injecting a test charge. All the HPD modules worked well and the electronics channels showed stable gains over the whole flight. Pedestal runs were taken automatically every 5 min in order to monitor the temperature drift of pedestals (about 12 ADC/°C on average) and perform accurate pedestal subtraction to all the physics data. Fig. 2(a) shows the typical temporal behaviour of the pedestals of one HPD: the oscillation reflects the 24-h temperature cycle. The average pedestal noise during the flight showed small fluctuations around the value of 1.2 ADC (Fig. 2(b)), in good agreement with previous laboratory measurements (Lee et al., 2005). Only 14 channels out of 2560 were found to have a pedestal rms noise larger than 3 ADC counts, while 5 channels were inefficient. The inclusive pulse height spectra of all the cells of a calorimeter plane are shown in Fig. 3, where the histograms in the top panel (a) refer to channels corresponding to the LOW portion of the dynamic range, while those in (b) belong to the MID range. Each layer is readout by two different HPD modules located on opposite sides of the calorimeter. The pulse height distribution from the 25 even (odd) numbered ribbons in a half-layer are
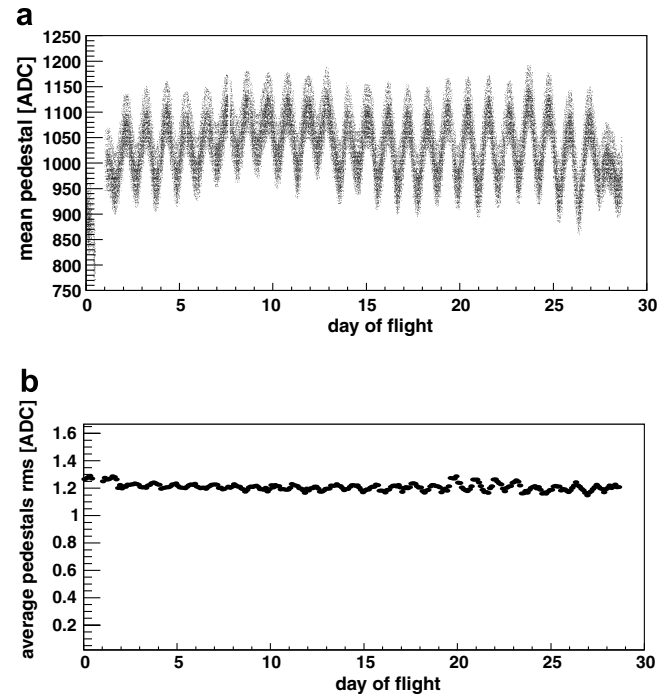
Fig. 2. (a) Pedestal values of the channels of one HPD vs. day of flight. (b) Calorimeter average pedestal rms noise during the flight.
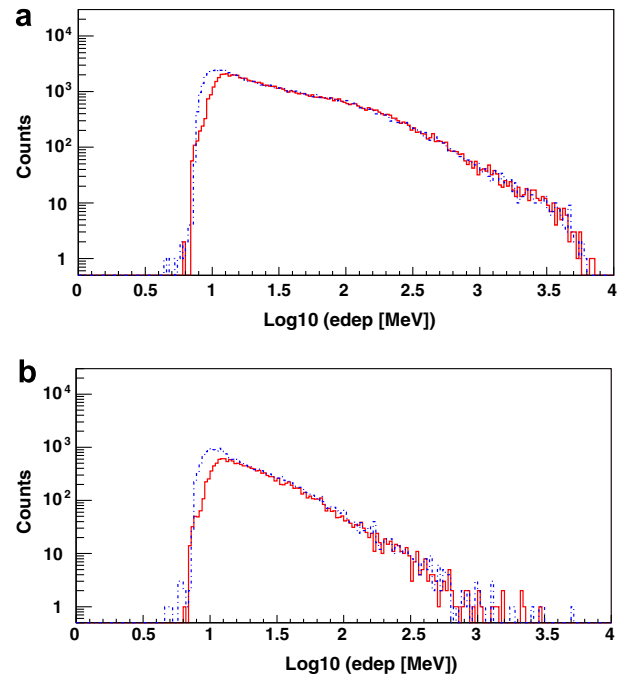
Fig. 3. Calorimeter pulse height distributions from the even (dashed line) and odd (continuous line) numbered cells of one calorimeter layer. Low-range and middle-range channels are shown, respectively, in (a) and (b).

shown as dashed (continuous) line. The LOW range channels spectra show a lower and an upper cutoff at ADC values close to 0.7 and 3.5, respectively (in Log_{10} scale). The first one is due to the in-flight sparsification threshold, while the upper cut marks the end of the 12 bit dynamic range of the ADC. The shape of the LOW and MID spec-

tra reflects the power law spectrum of the incident particles. However, the effect of the calorimeter threshold (around 60 MeV) is visible on the LOW range distribution, with a departure from a power law for signals below ∼100 MeV.

3.2. The silicon charge detector

The SCD, described in more detail elsewhere (Park et al., 2004), is a double array of silicon sensors designed to provide a charge identification of the incident nucleus. This task is achieved via an accurate measurement of its electric charge Z, taking advantage of the Z^2 dependence of specific ionization in the silicon sensor. The latter is a 4×4 matrix of PIN pixel diodes with an active area of 2.1 cm^2. The sensors are arranged in two layers separated by a vertical distance of about 4 cm. Each layer has a seamless active area of 0.52 m^2. During the CREAM-2 flight, a total of 2496 channels per layer were readout (Zinn et al., 2005), with only 0.8% (0.2%) of pixels from the bottom (top) SCD layer which were masked off.

3.3. The timing charge detector and Cherenkov counter

The timing charge detector (TCD) (Beatty et al., 2003) consists of two layers of 4 slabs each of 5 mm-thick plastic scintillators, at the top of the CREAM instrument, covering an area of 120×120 cm^2. The amplitude and time profile of light pulses are measured with fast photomultiplier tubes at either end of each scintillator. A hodoscope of scintillating fibers, known as S3, is located immediately above the calorimeter, to provide a reference time for the TCD. The small time-of-flight difference between the scintillation signal in the TCD from the incident nucleus, and the delayed signal from back-scattered particles from interactions in the calorimeter, is used to reject this type of background. The TCD systems for the CREAM-2 instrument performed well throughout the 28-day flight, with a performance comparable to that for the 42-day CREAM-1 flight (Coutu et al., 2007).

The Cherenkov detector, covering the same area as the TCD, is a 1 cm-thick plastic radiator readout by eight photomultiplier tubes via wavelength shifting bars. It is used to flag relativistic nuclei and to provide a charge measurement supplemental to the one from the TCD.

4. The trigger

A detailed description of the trigger system and its implementation during the second flight is beyond the scope of this paper. For a discussion of the preliminary analysis reported herein, it is sufficient to consider three main trigger types. The first one, known as "CAL" trigger discriminates against the abundant low energy cosmic ray flux, by requiring the detection of a shower in the calorimeter. The topological cuts defining the minimal requirements for a shower are the presence of at least 6 consecutive calorimeter layers, with at least one hit per layer above a given threshold. During most of the flight, the latter was set around a value equivalent to 60 MeV energy deposit in one ribbon.

The second ("CAL and ZLO") and third ("CAL and ZHI") trigger types, required, as an additional condition, the presence of a significant ionization deposit in the TCD, consistent with the one expected from a low-Z or high-Z nucleus, respectively. For the former trigger, the threshold was set at an equivalent particle charge well below the proton, while for the latter the threshold was set above the proton, but below helium.

During the flight, diurnal variations of the "CAL trigger" rate were recorded with peak values observed in correspondence of the lowest balloon altitudes. The more restrictive "CAL and ZLO" and "CAL and ZHI" triggers did not show significant rate variations during the day–night cycle. Their average rates were ∼0.022 and 0.018 Hz, respectively.

5. Tracking particles with the calorimeter

The fine granularity of the calorimeter allows an accurate reconstruction of the shower axis. In each calorimeter layer, a cluster of hits around the ribbon with the maximum energy deposit is reconstructed. The position of a candidate track-point is then computed as the center-of-gravity of the cluster. The candidate track is built by matching candidate track-points along the same view. The shower axis parameters are calculated by a χ^2 fit. The reconstructed shower axis is back-projected to the SCD, where it is matched with the pixel hit by the incoming particle to provide a measurement of its charge. The reconstructed impact point of the extrapolated calorimeter track on a given SCD plane is affected by an error, which defines the width of a search region in the same plane. The pixels included within this area are scanned and the pixel with the maximum pulse height is selected (Ahn et al., 2005). For this procedure to be efficient, an accurate reconstruction of the impact point of the incident particle is essential.

The impact point of the calorimeter track on the SCD was compared with the position of the most energetic cluster in the same plane. The distribution of residuals is shown in Fig. 4, with an rms value of about 1 cm, in good agreement with MonteCarlo simulations (Ahn et al., 2001).

6. Charge identification in the SCD

Redundancy in the direct measurement of the electric charge of cosmic ray nuclei is provided in the CREAM-2 instrument by the SCD silicon arrays, the TCD scintillator paddles and the Cherenkov counter. The analysis of the data of the second flight from the latter two subsystems will be reported in a later paper.

Two-independent measurements of dE/dx are provided by the two layers of silicon sensors of the SCD. In order to discriminate the ionization produced by the incident particle against the background generated by low energy backsplash (mainly the result of back-scattering off the cal-
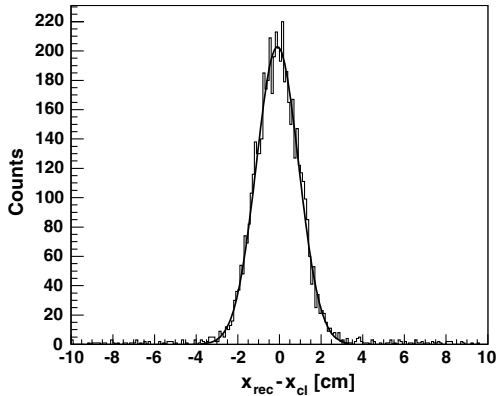
Fig. 4. Impact point residuals on the top SCD plane obtained with the calorimeter tracking for a selection of $Z > 4$ nuclei. The σ of the fitted gaussian is about 1 cm.

orimeter section), the granularity of the SCD had to be optimized. It had to be sufficiently small to allow for an unambiguous identification of the pixel hit by the imping-ing cosmic ray, yet the total number of readout channels had to remain limited. The SCD pixel size resulted from a tradeoff between the impact point resolution of calorim-eter showers on the silicon array plane (of order 1 cm) and a reasonable total number of readout channels (less than 3000 per layer).

While predominantly of charge $Z = 1$, the ionization from non relativistic albedo particles may be larger than the one expected from a mimimum ionizing particle. There-fore their apparent charge is distributed with values $Z \geqslant 1$ and can cause misidentification of the incoming nucleus. An efficient rejection of the back-scattered particles is already achieved by a correct match of the hit in the SCD with the back-projection of the calorimeter track, but additional powerful discrimination is provided by the correlation between the two-independent charge measure-ments from the two layers. After offline pedestal subtrac-tion and pulse height corrections, the signal from either SCD layer was corrected for the estimated path-length in the silicon, as calculated from the track parameters. The estimated charge was normalized to an absolute charge scale which was inferred from the flight data, by fitting the charge distributions of the CNO group. The signal matched with the track on the bottom SCD layer was then compared with the one matched on the upper layer and the values of their estimated charges were required to be con-sistent within 30%.

7. Energy measurement

7.1. Calorimeter energy calibration

The CREAM-2 calorimeter was calibrated with electron beams of 50, 100, 150, and 200 GeV in the H2 beam line at CERN in September 2004 (Marrocchesi et al., 2005). Data collected during the horizontal and vertical beam scans,

with 150 GeV electrons, were studied to equalize the calo-rimeter at channel level. A two step procedure was imple-mented in the calibration method described below. First, the response of each ribbon connected to a same HPD (averaged over about 5000 events) was obtained. Then, each group of 25 ribbon signals was equalized to the aver-age response of the respective half-layer. The second step of the procedure consisted in equalizing the individual aver-age response of the 40 HPDs. This was needed in order to take into account the differences in quantum efficiency (QE) and optical coupling among the photodetectors. This correction is not straightforward because the scintillation light collected by each HPD is a function of its depth in the Tungsten/Sci-Fi stack, at a given energy. Therefore, the dependence on the longitudinal shower profile of the HPD average responses had to be factorized out. This method was applied at one beam energy (150 GeV) where a set of energy independent constants, one per HPD, was extracted by comparing the longitudinal shower profile obtained with the 40 HPD average signals with the one pre-dicted by a Monte Carlo simulation based on the Fluka package (Fasso' et al., 2005).

The same procedure was then repeated with data sets taken at different energies, as a consistency check of the energy independence of the HPD equalization constants. Application of the calibration constants to the data taken at different beam energies resulted in an average longitudi-nal profiles in agreement with the simulations (Fig. 5).

7.2. Energy measurement from the sampling calorimeter

The energy deposit in the cells of the calorimeter were scaled according to the actual value of the high voltage during the flight. LOW and MID scales were inter-cali-brated using the flight data; the middle-range signal of each ribbon was used whenever the corresponding low-range signal deviated from linearity due to saturation of the dynamic range of the front-end electronics. The total energy sampled by the calorimeter was obtained by sum-ming up the calibrated values of all cells of the calorimeter,
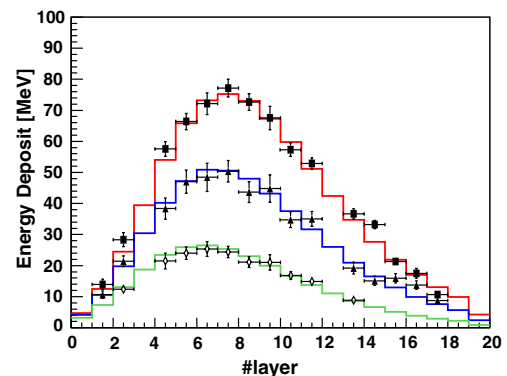

Fig. 5. Calorimeter calibration. Data points: average longitudinal profiles with electrons of 50, 100, and 150 GeV during CERN beam test. Solid line: MonteCarlo prediction.

selecting the appropriate range (low or middle) for each channel, on an event-by-event basis.

The energy of the incoming cosmic ray can be related to the sampled energy recorded in the calorimeter. The sampling fractions for protons and heavy nuclei up to Fe (and above) were studied with the CREAM-1 calorimeter at CERN with $A/Z = 2$ nuclei at 158 GeV/n beam energy (Ahn et al., 2006). Furthermore, the data from the first flight can be used to intercalibrate the calorimeter energy scale with the TRD on a subset of nuclei. The study of the absolute energy scale calibration, with data from both flights, will be reported in a later paper.

8. Event selection and fiducial volume

The preliminary analysis of the second flight data reported in this paper, was performed on a sample of good runs taken in the period December 19, 2005–January 12, 2006, when a total number of about 3×10^6 CAL triggers were recorded. Events were selected if the reconstructed incoming particle was contained inside a fiducial volume. Regions were chosen in the SCD and in the calorimeter where corrections for instrumental effects near the boundary of the active region of each detector could be neglected. The fiducial area on the upper SCD plane and the entrance window of the calorimeter were limited in this analysis to 64×64 and 40×40 cm², respectively. The acceptance cut requires one track to fall inside the fiducial volume within error ($\pm 1\sigma$), as calculated from the extrapolation of the reconstructed calorimeter shower to the region of interest. Events were further selected requiring not less than 6 consecutive calorimeter layers to be found with at least one hit per layer. Application of the above "software trigger" condition in the offline analysis, removed very efficiently spurious events, triggered by instrumental noise, with no showers in the calorimeter. This was confirmed by a visual scan of a sample of discarded events. Alternatively, spurious events triggered by the calorimeter background noise (trigger type "CAL" with no trigger flag from TCD) could be removed by requiring a well reconstructed shower (χ^2 cut from the shower fit).

9. Observed charge distribution in the SCD

The preliminary charge distributions shown in Fig. 6(a) (proton and He candidates) and Fig. 6(b) (candidate nuclei with $4 < Z < 15$), were obtained, with the above event selection, by matching the back-projected shower axis reconstructed in the calorimeter to the nearest pixel of each SCD plane and by requiring a consistent charge assignment from both planes. The above distributions are not representative of cosmic ray composition, but provide information about the level of purity that can be achieved by a preliminary exclusive selection of nuclei candidates based on simple charge cuts.

The distributions of p and He candidates in Fig. 6(a) were fitted with a Landau distribution convoluted with a
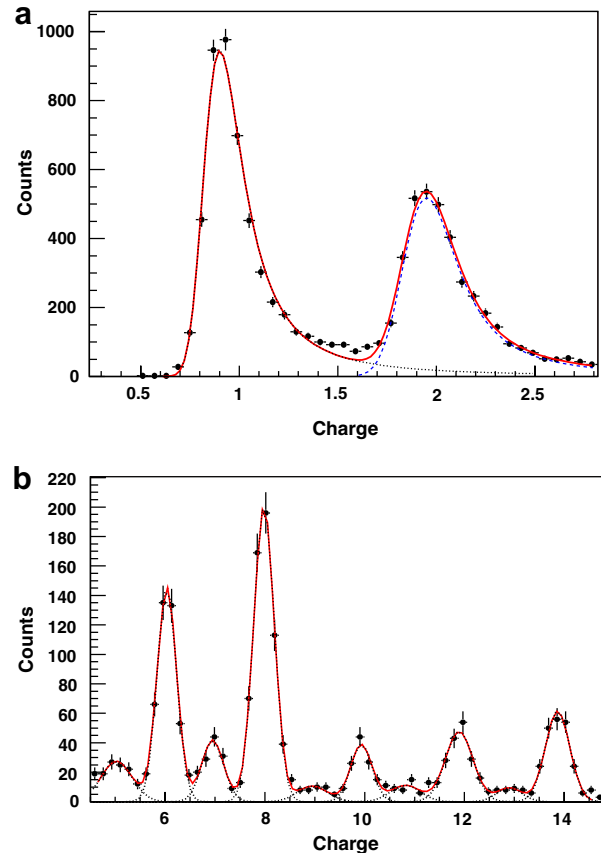

Fig. 6. Preliminary charge reconstruction of relativistic nuclei by the SCD using calorimeter tracking (the distributions are only indicative of the instrument charge resolution and relative elemental abundances are not meaningful): (a) candidate protons and He nuclei (solid line: result of the global fit, dotted lines: individual fitted components); (b) candidate nuclei with charge $Z > 4$.

Gaussian resolution function (dotted lines). The measured charges of high-Z nuclei candidates were found to be normally distributed, as expected.

10. Observed energy deposit

Fig. 7 shows a preliminary distribution of the total energy deposit in the calorimeter in MeV units. All particles charges are included in the distribution which extends to values with a sampled energy larger than 100 GeV. Since the sampling fraction of the calorimeter for hadrons is of order 0.1%, this indicates that events were collected above 100 TeV total particle energy. These events were individually scanned. The power-law behaviour, expected from the energy dependence of the differential cosmic rays spectrum, is visible in the right-hand side of the distribution (values above 3.5 in Log_{10} scale). The calorimeter energy threshold and other instrumental effects are responsible for the shape of the curve on the lower energy side, with a deviation from a pure power-law. No corrections for these effects are applied in Fig. 7.
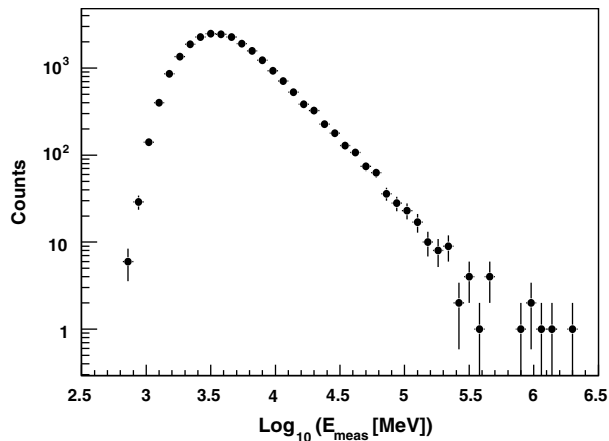
Fig. 7. Preliminary distribution of energy deposit [MeV] in the calorimeter (inclusive sample of incident nuclei: no selection on charge).

11. Conclusions

After no more than six months from the end of the second flight, a preliminary analysis confirms a stable and efficient performance of the instrument during the 28 days of permanence in the stratosphere. The quality of the data suggests that accurate results on the exclusive spectra and elemental composition of cosmic rays from CREAM are at hand.

Acknowledgements

References

Ahn, H.S., Beach, S., Beatty, J.J. Cosmic ray energetics and mass: expected performance, in: Proc. 27th Int. Cosmic Ray Conf., Hamburg, vol. 6, pp. 2159–2162, 2001.

Ahn, H.S., Bagliesi, M.G., Beatty, J.J., et al. Performance of CREAM calorimeter: results of beam tests, in: Proc. 9th Topical Seminar on Innovative Particle and Radiation Detectors (Siena), Nuclear Physics B (Proc. Suppl.), vol. 150, pp. 272–275, 2006.

Ahn, H.S., Allison, P., Bagliesi, M.G. CREAM flight data processing, in: Proc. 29th Int. Cosmic Ray Conf., Pune, vol. 3, pp. 389–392, 2005.

Beatty, J.J., Ahn, H.S., Allison, P., et al. The cosmic ray energetics and mass (CREAM) experiment timing charge detector, in: Proc. SPIE, vol. 4858: Particle Astrophysics Instrumentation, 4858, pp. 248–253, 2003.

Berezhko, E.G., Ksenofontov, L.T., Ptuskin, V.S., et al. Cosmic ray production in supernova remnants including reacceleration: the secondary to primary ratio. Astron. Astrophys. 410, 189–198, 2003.

Biermann, P.L. The spectrum and chemical composition above 10^4 GeV. Astron. Astrophys. 271, 649–658, 1993.

Lagage, P.O., Cesarsky, C.J. Cosmic ray shock acceleration in the presence of self-excited waves. Astron. Astrophys. 118, 223–228, 1983.

Coutu, S., Ahn, H.S., Allison, P., et al., Design and performance in the first flight of the transition radiation detector and charge detector of the CREAM ballon instrument, Proc. 10th Pisa Meeting on Advanced Detectors, Nucl. Instrum. Methods. A572, 485–487, 2007.

Fasso', A., Ferrari, A., Ranft, J., et al. FLUKA: a multi-particle transport code, *CERN*–2005–10, 2005.

Ganel, O., Seo, E.S., Ahn, H.S. Cosmic-ray energetics and mass: configuration and progress on costruction and testing, in: Proc. 27th Int. Cosmic Ray Conf., Hamburg, vol. 6, pp. 2163–2166, 2001.

Hillas, A.M. Can diffusive shock acceleration in supernova remnants account for high-energy galactic cosmic rays? J. Phys. G: Nucl. Partic. Phys. 31, R95–R131, 2005.

Lee, M.H., Ahn, H.S., Ganel, O., et al. Electronics for the CREAM calorimeter and hodoscopes. Proc. 29th Int. Cosmic Ray Conf., Pune 3, 409–412, 2005.

Marrocchesi, P.S., Ahn, H.S., Bagliesi, M.G., et al. Construction and test of a Tungsten/Sci-Fi imaging calorimeter for the CREAM experiment. Nucl. Instrum. Methods A535, 143–146, 2004.

Marrocchesi, P.S., Ahn, H.S., Bagliesi, M.G., et al. Beam test calibration of the balloon-borne imaging calorimeter for the CREAM experiment. Proc. 29th Int. Cosmic Ray Conf., Pune 3, 309–312, 2005.

Park, I.H., Ahn, H.S., Bok, J.B., et al. Heavy ion beam test results of the silicon charge detector for the CREAM cosmic ray balloon mission. NIM A535, 158–161, 2004.

Ptuskin, V.S. Cosmic ray propagation in the Galaxy. Nuovo Ciment. C 19, 755, 1996.

Seo, E.S., Ahn, H.S., Beatty, J.J., et al. Cosmic-ray energetics and mass (CREAM) balloon project. Adv. Space Res. 33 (10), 1777–1785, 2004.

Seo, E.S. New Observations with CREAM. Proc. 29th Int. Cosmic Ray Conf., Pune 10, 185–198, 2005.

Seo, E.S., et al. CREAM: 70 days of flight from 2 launches in Antarctica, COSPAR 2006, PSB1-0027-06.

Swordy, S.P. The energy spectra and anisotropies of cosmic rays. Space Sci. Rev. 99, 85–94, 2001.

Wefel, J.P., Adams, J.H., Ahn, H.S., et al. Energy spectra of H and He from the ATIC-2 experiment. Proc. 29th Int. Cosmic Ray Conf., Pune 3, 105–108, 2005.

Zinn, S.Y., Ahn, H.S., Allison, P., et al. The data acquisition software system of the 2004/2005 CREAM experiment. Proc. 29th Int. Cosmic Ray Conf., Pune 3, 437–440, 2005.